

The Co-ordination Chemistry of Mixed Pyridine–Phenol Ligands; Synthesis of 6-(2-Hydroxyphenyl)-2,2'-bipyridine (HL) and the Crystal Structures of $[\text{Cu}_2\text{L}_2(\mu\text{-MeCO}_2)]\text{-}[\text{PF}_6]\cdot 1.5\text{CH}_2\text{Cl}_2$ and $[\text{CoL}_2][\text{PF}_6]\cdot \text{MeCN}^\dagger$

John C. Jeffery, Erik Schatz and Michael D. Ward*
School of Chemistry, Cantock's Close, Bristol BS8 1TS, UK

The new N,N,O-tridentate ligand 6-(2-hydroxyphenyl)-2,2'-bipyridine (HL) has been prepared in 41% yield overall by reaction of 2-lithioanisole with 2,2'-bipyridine, followed by rearomatisation with KMnO_4 and subsequent conversion of the anisole group to a phenol with pyridinium hydrochloride. Complexes with Co^{III} , Ni^{II} and Cu^{II} have been prepared, which possess different structures and metal:ligand ratios. The structure of $[\text{CoL}_2][\text{PF}_6]\cdot \text{MeCN}$, established by X-ray diffraction, is mononuclear with a near octahedral *cis*- N_4O_2 co-ordination sphere; the presence of the phenolates stabilises the Co^{III} oxidation state by about one volt relative to $[\text{Co}(\text{terpy})_2]^{3+}$ (terpy = 2,2':6',2''-terpyridine). The crystal structure of $[\text{Cu}_2\text{L}_2(\mu\text{-MeCO}_2)][\text{PF}_6]\cdot 1.5\text{CH}_2\text{Cl}_2$ shows two near-planar CuL fragments stacked adjacent to each other such that the coplanar aromatic rings of the ligands are separated by an average of 3.54 Å, comparable to the stacking distances in graphite and nucleic acids. Both phenolate residues and the acetate bridge the two copper(II) centres, giving a $\text{Cu}_2(\mu\text{-O})_2(\mu\text{-1,3-MeCO}_2)$ core. By contrast the nickel(II) complex has the formulation $[\text{NiL}_2]\cdot \text{HPF}_6$.

Polydentate chelating ligands based on polypyridines have been very popular targets of study recently and have played a major role in the current intense interest in co-ordination chemistry. Significant recent areas of research include the spontaneous self-assembly of polynuclear double-helical complexes based on long, flexible polypyridine ligands;^{1,2} the development of bipyridine and terpyridine analogues containing other heterocyclic donors, such as 2-phenylpyridine [a C,N-donor analogue of bipy (2,2'-bipyridine)] and 2-thienylbipyridine [an N,N,S-donor analogue of terpy (2,2':6',2''-terpyridine)];³ and the photochemical and photo-physical properties of polynuclear ruthenium(II) complexes with polypyridine ligands, and their potential use in photochemical devices.⁴

The co-ordination chemistry of polydentate chelating ligands containing a mixture of pyridine and phenol donors is one possible extension to the chemistry of polypyridines which has received very little attention. Such ligands may be expected to stabilise higher oxidation states than their polypyridine counterparts, due to substitution of one (or more) π -accepting pyridyl groups by σ -donating phenol groups; the presence of six-membered rather than five-membered chelate rings in the complexes may also lead to altered geometries. A few years ago⁵ it was reported that 2-(2-hydroxyphenyl)pyridine, an N,O-bidentate donor, forms a normal tris-chelate octahedral complex with cobalt(III) and a bis-chelate square-planar complex with palladium(II), and there is an erroneous (see below) early report⁶ of the synthesis of the O,N,N,O-tetradentate ligand 6,6'-bis-(2-hydroxyphenyl)-2,2'-bipyridine. We now report the synthesis of 6-(2-hydroxyphenyl)-2,2'-bipyridine (HL), an N,N,O-terdentate terpy analogue, and the structures and spectroscopic properties of its mononuclear complex with cobalt(III) and binuclear phenolate-bridged complex with copper(II).

Experimental

NMR spectra were recorded on JEOL GX270 or GX400 spectrometers, electron-impact (EI) mass spectra on a Kratos MS9 instrument, fast-atom bombardment (FAB) mass spectra on a VG-ZAB instrument and UV/VIS spectra on a Perkin-Elmer Lambda 2 spectrophotometer. ESR spectra were recorded on a Bruker ESP-300E spectrometer. Room-temperature magnetic susceptibility measurements were performed with a Sherwood Scientific MSB-1 balance. Electrochemical experiments were performed using an EG&G PAR model 273A potentiostat. A standard three-electrode configuration was used, with platinum-bead working and auxiliary electrodes and a saturated calomel electrode (SCE) reference. Ferrocene was added at the end of each experiment as an internal standard; all potentials are quoted *vs.* the ferrocene-ferrocenium couple. The solvent was acetonitrile, purified by distillation twice from CaH_2 . The base electrolyte was 0.1 mol dm^{-3} $[\text{NBu}_4][\text{PF}_6]$. All solvents were dried by standard methods before use. 2,2'-Bipyridine and 2-bromoanisole were obtained from Aldrich and used as received.

Preparations.—6-(2-Methoxyphenyl)-2,2'-bipyridine. To an ice-cold solution of 2,2'-bipyridine (5.06 g, 32.4 mmol) in diethyl ether (100 cm^3) under nitrogen was added *via* a double-ended needle a solution of 2-lithioanisole (39 mmol, 20% excess), prepared from 2-bromoanisole (7.37 g, 39 mmol) and lithium (0.30 g, 43 mmol) in ether (50 cm^3). The resulting brown solution was allowed to warm to room temperature and stirred overnight. Water was then added *dropwise* with vigorous stirring until the effervescence ceased, and water (50 cm^3) was added. The deep yellow ether layer was separated and evaporated to dryness. The resulting oil was redissolved in acetone (50 cm^3), cooled in an ice-salt bath, and a saturated solution of KMnO_4 in acetone added *dropwise* until the purple colour persisted. The MnO_2 was removed by filtration through Celite, the solvent removed on a rotary evaporator, and the product isolated by chromatography on silica. Initially CH_2Cl_2 was used as eluent to remove traces of anisole or 2-

† Supplementary data available: see Instructions for Authors, *J. Chem. Soc., Dalton Trans.*, 1992, Issue 1, pp. xx–xxv.

Table 1 Analytical and spectroscopic data for the new complexes

Complex	Elemental analysis ^a (%)			FAB mass spectrum ^b <i>m/z</i> (assignment)	UV/VIS spectrum λ_{\max} (nm), $10^{-3} \epsilon/dm^3 \text{ mol}^{-1} \text{ cm}^{-1}$
	C	H	N		
[Cu ₂ L ₂ (μ -MeCO ₂)] [PF ₆] ^c	49.6 (49.5)	3.2 (3.0)	6.9 (6.8)	679 [Cu ₂ L ₂ (μ -MeCO ₂)] ⁺	635 (0.23), 378 (12), 316 (16), 282 (21), 234 (51)
[CoL ₂] [PF ₆] ^d	54.5 (55.0)	3.0 (3.2)	7.6 (8.0)	553 [CoL ₂] ⁺	583 (0.52), 372 (7.1), 314 (15), 257 (39), 229 (45), 215 (46)
[NiL ₂]·HPF ₆ ^c	55.1 (55.0)	3.7 (3.3)	7.9 (8.0)	1250 {[NiL ₂] ₂ [HPF ₆]} ⁺ 857 [Ni ₂ L ₃] ⁺ 553 [NiL ₂] ⁺	860 (0.018), 530 (sh) (0.024), ^e 314 (31), 270 (sh) (33), 220 (70)

^a Calculated values in parentheses. ^b Spectra recorded with 3-nitrobenzyl alcohol as matrix; all peaks have the correct isotopic pattern. ^c UV/VIS spectrum recorded in CH₂Cl₂. ^d UV/VIS spectrum recorded in MeCN. ^e sh = Shoulder.

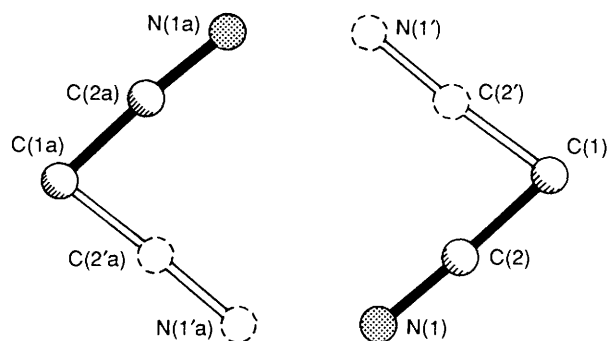


Fig. 1 Depiction of the disordered lattice acetonitrile molecule in [CoL₂][PF₆] \cdot MeCN

bromoanisole, then the polarity was steadily increased by addition of methanol (up to 5%, v/v in CH₂Cl₂) until the product eluted. 6-(2-Methoxyphenyl)-2,2'-bipyridine was obtained as a pale yellow oil (3.86 g, 45%). EI MS: $m/z = 261$ ($M^+ - H$). ¹H NMR (400 MHz, CDCl₃): δ 3.90 (3 H, s, OMe), 7.04 (1 H, d, $J = 8.3$, phenyl H⁶), 7.13 (1 H, td, $J = 7.6, 1.0$, phenyl H⁴), 7.30 (1 H, ddd, $J = 7.6, 4.9, 1.2$, H⁵), 7.40 (1 H, ddd, $J = 8.8, 6.9, 1.9$, phenyl H⁵), 7.81 (1 H, td, $J = 7.9, 1.8$, H⁴), 7.84 (1 H, t, $J = 7.8$, H⁴), 7.92 (1 H, dd, $J = 7.8, 1.2$, H³ or H⁵), 8.01 (1 H, dd, $J = 7.6, 1.9$, phenyl H³), 8.34 (1 H, dd, $J = 7.8, 1.0$, H⁵ or H³), 8.58 (1 H, d, $J = 8.1$, H³) and 8.69 (1 H, ddd, $J = 4.9, 1.8, 1.0$ Hz, H⁶) (Found: C, 77.6; H, 5.1; N, 10.9. Calc. for C₁₇H₁₄N₂O: C, 77.8; H, 5.4; N, 10.7%).

6-(2-Hydroxyphenyl)-2,2'-bipyridine (HL). This was prepared from 6-(2-methoxyphenyl)-2,2'-bipyridine by treatment with molten pyridinium chloride at 200 °C for 2 h under N₂ according to a published procedure.⁷ After cooling, the solid mass was dissolved in water and the pH adjusted to 7 with NaOH. The light brown precipitate was collected by filtration and dried *in vacuo*. Final purification was achieved by filtration through a short alumina column (Brockmann activity II) with CH₂Cl₂ as eluent. 6-(2-Hydroxyphenyl)-2,2'-bipyridine was isolated as a cream-coloured microcrystalline solid in 90% yield. EI MS: $m/z = 248$ (M^+). ¹H NMR (400 MHz, CDCl₃): δ 6.96 (1 H, td, $J = 7.0, 1.1$, phenyl H⁴), 7.07 (1 H, dd, $J = 8.1, 1.1$, phenyl H⁶), 7.33–7.40 (2 H, m, H⁵ and phenyl H⁵), 7.85–7.91 (2 H, m, H⁴ and phenyl H³), 7.95–8.03 (2 H, m, H⁴ and H³ or H⁵), 8.20 (1 H, d, $J = 8.1$, H³), 8.33 (1 H, dd, $J = 7.3, 1.3$, H⁵ or H³), 8.74 (1 H, d, $J = 3.8$ Hz, H⁶), 14.62 (1 H, s, phenolic OH). M.p. 103–104 °C (Found: C, 77.3; H, 5.1; N, 11.1. Calc. for C₁₆H₁₂N₂O: C, 77.4; H, 4.9; N, 11.3%).

[Cu₂L₂(μ -MeCO₂)] [PF₆] \cdot 1.5CH₂Cl₂, [CoL₂] [PF₆] \cdot MeCN and [NiL₂]·HPF₆. The complexes were prepared by reaction of HL with one equivalent of copper(II) acetate, 0.5 equivalent of cobalt(II) acetate or 0.5 equivalent of nickel(II) chloride respectively in methanol at room temperature for 30 min. Addition of an aqueous solution of KPF₆ to the dark

solutions precipitated the complexes. The cobalt and nickel complexes were recrystallised by diffusion of diethyl ether vapour into concentrated solutions; the copper complex was recrystallised by slow evaporation of a dichloromethane solution. Analytical and spectroscopic data are summarised in Table 1.

Crystal Structure Determinations.—Data were collected using a Siemens R3m/V four-circle diffractometer (293 K, Mo-K α X-radiation, graphite monochromator, $\lambda = 0.71073$ Å). The data were corrected for Lorentz, polarisation and X-ray absorption effects. The structures were solved by conventional heavy-atom or direct methods and successive Fourier difference syntheses were used to locate all non-hydrogen atoms. All calculations were performed on a DEC micro-Vax II computer with the SHELXTL PLUS system of programs.⁸ Scattering factors with corrections for anomalous dispersion were taken from ref. 9.

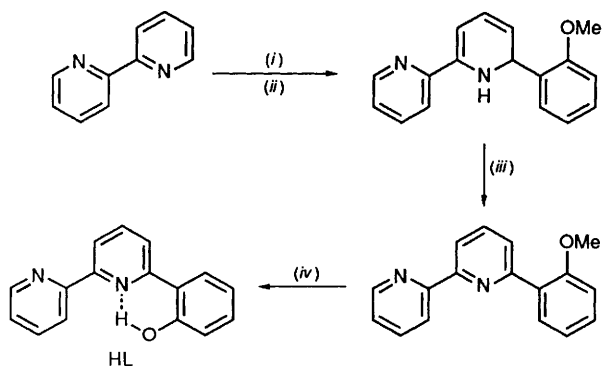
Additional material available from the Cambridge Crystallographic Data Centre comprises H-atom coordinates, thermal parameters and remaining bond lengths and angles.

Structure Determination of [CoL₂][PF₆] \cdot MeCN.—The crystal used for data collection (dimensions *ca.* 0.50 \times 0.25 \times 0.18 mm) was cut from a much larger crystal. Of the 5834 data collected (Wyckoff ω scans, $2\theta \leq 50^\circ$), 4178 unique data had $F \geq 5\sigma(F)$, and only these were used for structure solution and refinement. An empirical absorption correction was applied using a method based upon azimuthal scan data.

Crystal data for C₃₂H₂₂CoF₆N₄O₂P \cdot MeCN, $M = 739.5$, triclinic, space group $P\bar{1}$, $a = 11.909(6)$, $b = 12.573(6)$, $c = 12.917(6)$ Å, $\alpha = 114.02(3)$, $\beta = 102.23(4)$, $\gamma = 106.08(4)^\circ$, $U = 1577(1)$ Å³, $Z = 2$, $D_c = 1.56$ g cm⁻³, $F(000) = 752$, $\mu(\text{Mo-K}\alpha) = 6.7$ cm⁻¹.

All non-hydrogen atoms were refined with anisotropic thermal parameters. Hydrogen atoms were included in calculated positions (C–H 0.96 Å) with fixed isotropic thermal parameters ($U_{\text{iso}} = 0.08$ Å²). Final $R = 0.056$ ($R' = 0.060$) with a weighting scheme of the form $w^{-1} = [\sigma^2(F) + 0.0005F^2]$. The final electron density difference synthesis showed no peaks > 1.40 or < -0.63 e Å⁻³. The asymmetric unit contains one molecule of MeCN per molecule of the complex. The solvent molecule is disordered about an inversion centre and the nature of the disorder is shown in Fig. 1. The Me carbon atom C(1) occupies a fixed location but the atoms C(2) and N(1) each occupy two sites with occupancies of 0.68 and 0.32 respectively. The minor components of the disorder are indicated by primes and atoms generated by symmetry are given the suffix a.

Structure Determination of [Cu₂L₂(μ -MeCO₂)] [PF₆] \cdot 1.5CH₂Cl₂. Crystals were grown from CH₂Cl₂ and that used had dimensions *ca.* 0.60 \times 0.25 \times 0.20 mm. Of the 7245 data



Scheme 1 (i) 2-Lithioanisole, Et₂O; (ii) water; (iii) KMnO₄, acetone; (iv) pyridinium hydrochloride, 200 °C, 2 h

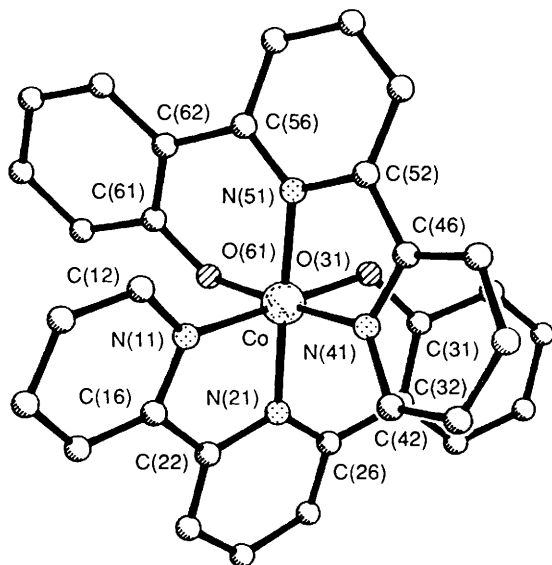


Fig. 2 Structure of the cation [CoL₂]⁺ showing the atom numbering scheme

collected (Wyckoff ω scan, $2\theta \leq 50^\circ$), 4203 unique data had $F \geq 6\sigma(F)$, and only these were used for structure solution and refinement. An empirical absorption correction was applied using a method based upon azimuthal scan data.

Crystal data for C₃₄H₂₅Cu₂F₆N₄O₄P·1.5CH₂Cl₂, $M = 953.0$, triclinic, space group $P\bar{1}$, $a = 8.000(2)$, $b = 15.490(5)$, $c = 16.911(6)$ Å, $\alpha = 107.95(3)$, $\beta = 99.67(3)$, $\gamma = 103.48(2)^\circ$, $U = 1872(1)$ Å³, $Z = 2$, $D_c = 1.69$ g cm⁻³, $F(000) = 958$, $\mu(\text{Mo-K}\alpha) = 14.7$ cm⁻¹.

All non-hydrogen atoms were refined with anisotropic thermal parameters. Hydrogen atoms were included in calculated positions (C–H 0.96 Å) with fixed isotropic thermal parameters ($U_{\text{iso}} = 0.08$ Å²). Final $R = 0.043$ ($R' = 0.045$) with a weighting scheme of the form $w^{-1} = [\sigma^2(F) + 0.0005F^2]$. The final electron density difference synthesis showed no peaks > 0.49 or < -0.52 e Å⁻³. The asymmetric unit contains 1.5 molecules of CH₂Cl₂ per molecule of the complex. One molecule of CH₂Cl₂ lies in a general position and is ordered, whilst the half molecule is disordered about an inversion centre. Hydrogen atoms were not included for the disordered CH₂Cl₂ molecule.

Results and Discussion

Synthesis of the new ligand HL was accomplished according to the method outlined in Scheme 1. Reaction of excess 2-lithioanisole with bipy in diethyl ether at room temperature followed by oxidation of the intermediate dihydrobipyridine with KMnO₄ in acetone gave a 45% yield of 6-(2-methoxy-

phenyl)-2,2'-bipyridine as a pale yellow oil; such additions of alkylolithium or aryllithium reagents to the C⁶ position of bipy and other polypyridines are well known.^{7,10} Conversion of the anisole group to a phenol was accomplished in 90% yield by demethylation using molten pyridinium chloride.⁷ Both 6-(2-methoxyphenyl)-2,2'-bipyridine and HL were fully characterised by elemental analyses, mass spectrometry and ¹H NMR spectrometry. Both NMR spectra contain eleven resonances in the aromatic region, which were assigned on the basis of two-dimensional ¹H–¹H correlation (COSY) spectra; the only ambiguity is that the two doublets due to H³ and H⁵ on the central pyridine ring cannot be uniquely assigned. The very high chemical shift (δ 14.62) of the phenolic proton of HL suggests a cisoid arrangement of the central pyridyl and terminal phenol rings, leading to an intramolecular hydrogen-bonding interaction as shown in Scheme 1. In keeping with this is the surprisingly low polarity of HL; during chromatographic purification of HL it was noticed that it elutes ahead of its precursor 6-(2-methoxyphenyl)-2,2'-bipyridine, which is directly contrary to the behaviour of anisole and phenol.

In an earlier (1946) report⁶ of the reaction between bipy and 2-lithioanisole, the authors assumed that addition of 2-lithioanisole occurred at each of the two bipy-C⁶ sites to give 6,6'-bis(2-methoxyphenyl)-2,2'-bipyridine. We found that even with a large excess of 2-lithioanisole, substitution occurs only once to give 6-(2-methoxyphenyl)-2,2'-bipyridine, and no trace of 6,6'-bis(2-methoxyphenyl)-2,2'-bipyridine could be detected in the reaction mixture. The only characterisation of the supposed 6,6'-bis(2-methoxyphenyl)-2,2'-bipyridine consisted of elemental analyses for carbon and hydrogen on the demethylated material; although the figures quoted are consistent with the formation of 6,6'-bis(2-hydroxyphenyl)-2,2'-bipyridine, by coincidence they are also consistent with the formation of the *mono*-substituted product HL. In addition, the melting point we obtained for HL (103–104 °C) is virtually identical to that reported for the supposed 6,6'-bis(2-hydroxyphenyl)-2,2'-bipyridine (102.5–103.5 °C). It seems certain therefore that, lacking modern spectroscopic techniques, the report of the synthesis of 6,6'-bis(2-hydroxyphenyl)-2,2'-bipyridine was mistaken and HL was actually prepared.

Reaction of HL with half an equivalent of cobalt(II) acetate in methanol in the presence of air quickly gave a dark green-brown solution, from which a green-brown solid was precipitated by addition of KPF₆ and recrystallised from acetonitrile–diethyl ether. The FAB mass spectrum and the elemental analysis figures are consistent with the formation of the cobalt(III) complex [CoL₂][PF₆] by facile aerial oxidation.

The crystal structure has been determined, and the structure of the complex cation is shown in Fig. 2; relevant bond lengths and angles are in Table 2, and atomic coordinates in Table 3. The geometry, as would be expected for Co^{III}, is near octahedral with the two inequivalent, deprotonated ligands binding meridionally. On comparison with the structure of [Co(terpy)₂]³⁺¹¹ significant differences are revealed. In [Co(terpy)₂]³⁺ the terpy ligands, with their five-membered chelate rings, do not have a large enough bite to give ideal octahedral geometry. This results in the bonds to the terminal pyridyl N atoms (1.92–1.94 Å) being about 0.07 Å longer than the bonds to the central pyridyl N atoms (1.85–1.86 Å), and a bite of 164° between the terminal N atoms of each terpy ligand. The terpy ligands are nearly planar, with torsion angles of 1.9–4.4° between rings. In [CoL₂][PF₆], the presence of a six-membered chelate ring in each ligand allows them to approach the octahedral geometry required by the metal centre without undue strain. The bite angles between the terminal N and O atoms of each ligand are 176.8(2) and 178.5(2)°, and the bonds to the central N atoms are now not compressed relative to the bonds to the terminal N atoms. In order to accommodate the extra size of the six-membered chelate rings and the (formal) sp³ hybridisation of the oxygen atoms, the two ligands L are considerably distorted from planarity. In one ligand there is a

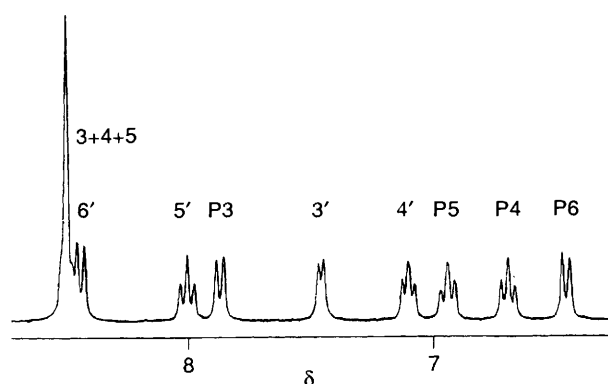


Fig. 3 400 MHz ^1H NMR spectrum of $[\text{CoL}_2][\text{PF}_6]$ in CD_3CN at 20°C ; chemical shifts are vs. internal SiMe_4 . The letter 'P' in the assignments denotes the phenyl ring

Table 2 Selected internuclear distances (Å) and angles ($^\circ$) for the complex $[\text{CoL}_2][\text{PF}_6]\cdot\text{MeCN}$

Co–N(11)	1.912(4)	Co–O(61)	1.886(4)
Co–N(51)	1.914(5)	Co–O(31)	1.869(3)
Co–N(21)	1.923(5)	Co–N(41)	1.925(4)
N(11)–Co–N(21)	84.4(2)	Co–N(11)–C(16)	113.6(4)
N(11)–Co–N(41)	92.3(2)	Co–N(21)–C(26)	126.3(3)
N(11)–Co–N(51)	97.0(2)	Co–N(41)–C(42)	128.2(4)
N(41)–Co–N(51)	83.1(2)	Co–N(51)–C(52)	112.8(3)
O(31)–Co–O(61)	89.8(1)	Co–O(61)–C(61)	120.3(4)
Co–N(11)–C(12)	127.6(4)	N(21)–Co–O(31)	94.9(2)
Co–N(21)–C(22)	113.0(4)	O(31)–Co–N(41)	89.1(2)
Co–O(31)–C(31)	124.5(2)	O(31)–Co–N(51)	83.7(2)
C(42)–N(41)–C(46)	118.6(5)	N(21)–Co–O(61)	87.3(2)
C(52)–N(51)–C(56)	120.6(5)	N(51)–Co–O(61)	93.8(2)
N(11)–Co–O(31)	178.5(2)	C(12)–N(11)–C(16)	118.7(4)
N(21)–Co–N(41)	95.8(2)	C(22)–N(21)–C(26)	120.5(5)
N(21)–Co–N(51)	178.3(2)	Co–N(41)–C(46)	113.2(3)
N(11)–Co–O(61)	88.8(2)	Co–N(51)–C(56)	125.5(4)
N(41)–Co–O(61)	176.8(2)		

Table 3 Atomic coordinates ($\times 10^4$) for $[\text{CoL}_2][\text{PF}_6]\cdot\text{MeCN}$

Atom	x	y	z	Atom	x	y	z
Co	1 556(1)	3 753(1)	1 968(1)	N(51)	1 459(3)	2 231(3)	2 019(3)
N(11)	3 349(3)	4 607(3)	2 635(3)	C(52)	1 002(4)	2 115(4)	2 862(4)
C(12)	4 190(5)	4 202(5)	3 050(5)	C(53)	559(5)	966(5)	2 843(5)
C(13)	5 443(5)	4 867(6)	3 429(6)	C(54)	592(5)	–79(5)	1 932(5)
C(14)	5 898(5)	5 984(6)	3 383(7)	C(55)	1 111(5)	38(4)	1 119(5)
C(15)	5 044(5)	6 405(5)	2 975(6)	C(56)	1 589(4)	1 240(4)	1 182(4)
C(16)	3 783(4)	5 710(4)	2 607(4)	O(61)	1 616(3)	3 127(3)	392(3)
N(21)	1 609(3)	5 279(3)	1 930(3)	C(61)	2 207(4)	2 369(4)	45(4)
C(22)	2 781(4)	6 079(4)	2 183(4)	C(62)	2 221(4)	1 443(4)	382(4)
C(23)	3 014(5)	7 166(5)	2 111(5)	C(63)	2 855(5)	681(5)	–61(5)
C(24)	1 997(5)	7 418(5)	1 707(5)	C(64)	3 429(6)	783(6)	–825(6)
C(25)	814(5)	6 608(4)	1 435(4)	C(65)	3 418(6)	1 689(6)	–1 177(6)
C(26)	600(4)	5 538(4)	1 588(4)	C(66)	2 822(6)	2 479(6)	–736(5)
O(31)	–198(3)	2 918(3)	1 278(3)	P	5 048(2)	1 279(2)	3 542(2)
C(31)	–972(4)	3 499(4)	1 289(4)	F(1)	4 705(10)	–40(5)	2 679(11)
C(32)	–653(4)	4 728(4)	1 402(4)	F(2)	3 732(5)	1 195(10)	3 203(9)
C(33)	–1 635(5)	5 144(5)	1 279(5)	F(3)	5 444(6)	2 753(6)	4 407(7)
C(34)	–2 831(5)	4 432(6)	1 091(6)	F(4)	6 437(6)	1 527(7)	3 881(9)
C(35)	–3 122(5)	3 259(5)	1 028(5)	F(5)	4 867(11)	969(11)	4 483(9)
C(36)	–2 202(4)	2 811(5)	1 136(5)	F(6)	5 300(8)	1 773(7)	2 656(7)
N(41)	1 466(3)	4 298(3)	3 562(3)	C(1)	7 752(12)	84(17)	5 016(14)
C(42)	1 732(4)	5 486(4)	4 430(4)	C(2)	8 976(23)	881(15)	5 571(15)
C(43)	1 659(5)	5 753(5)	5 543(5)	N(1)	10 070(18)	1 571(12)	6 042(13)
C(44)	1 251(5)	4 755(5)	5 776(5)	C(2')	8 279(28)	–678(34)	4 423(26)
C(45)	977(5)	3 539(5)	4 905(5)	N(1')	8 610(26)	–1 472(25)	3 929(25)
C(46)	1 108(4)	3 331(4)	3 804(4)				

torsion angle of 1.9° between the pyridyl rings and one of 14.5° in the opposite sense between the central pyridine ring and the phenolate ring; in the other ligand these torsion angles are 9.1° and 28.9° respectively, with the same change of sense between them. These pyridine–phenolate torsion angles are comparable to those in the cobalt(III) complex of 2-(2-hydroxyphenyl)pyridine, which vary between 22 and 29° .⁵ The wide variation in this parameter suggests that the rotational energy barrier is low and that the magnitude of the torsion angle may be strongly influenced by crystal packing forces. This is confirmed by the ^1H NMR spectrum of $[\text{CoL}_2][\text{PF}_6]$ (Fig. 3) which clearly shows only eleven resonances in the aromatic region, indicating that the two ligands are equivalent in solution; the assignments were made on the basis of a COSY spectrum.

Cyclic voltammetry of $[\text{CoL}_2][\text{PF}_6]$ in acetonitrile (Fig. 4) shows a quasi-reversible reduction centred at -0.90 V vs. ferrocene–ferrocenium (ΔE_p varies from 130 mV at a scan rate of 20 mV s^{-1} to 230 mV at a scan rate of 2 V s^{-1} ; $i_{pa} \approx i_{pc}$). Coulometry confirmed that this is a one-electron reduction; a bulk electrolysis with a platinum gauze working electrode at -1.1 V vs. ferrocene–ferrocenium resulted in a colour change from dark green-brown to a much paler orange-brown, indicating that the reduction is a metal-centred $\text{Co}^{\text{III}}\text{--Co}^{\text{II}}$ reduction. Estimates of the value of the $\text{Co}^{\text{III}}\text{--Co}^{\text{II}}$ redox couple in $[\text{Co}(\text{terpy})_2]^{3+}$ vary according to the experimental conditions¹² but it is clear that, as expected, substitution of two pyridine donors by phenolates results in stabilisation of the Co^{III} state by about one volt. A $\text{Co}^{\text{II}}\text{--Co}^{\text{I}}$ couple was not apparent within the potential window permitted by the solvent. The voltammogram also shows a totally irreversible oxidation, presumably ligand based, at $+0.87$ V vs. ferrocene–ferrocenium. The UV/VIS spectral details for $[\text{CoL}_2][\text{PF}_6]$ are summarised in Table 1. The $^1\text{T}_{1g} \rightarrow ^1\text{A}_{1g}$ d–d transition occurs at 583 nm, in contrast to the equivalent absorption for $[\text{Co}(\text{terpy})_2]^{3+}$ which is at 444 nm;¹³ this is a consequence of the lower ligand-field strength of phenolates compared to pyridines, and explains the intense colour of the complex. In the UV region the spectrum is dominated by phenolate– Co^{III} charge-transfer bands and ligand-based $\pi\text{--}\pi^*$ transitions.

Reaction of HL with one equivalent of copper(II) acetate in methanol quickly resulted in a clear bottle-green solution. Addition of KPF_6 precipitated a green solid which was

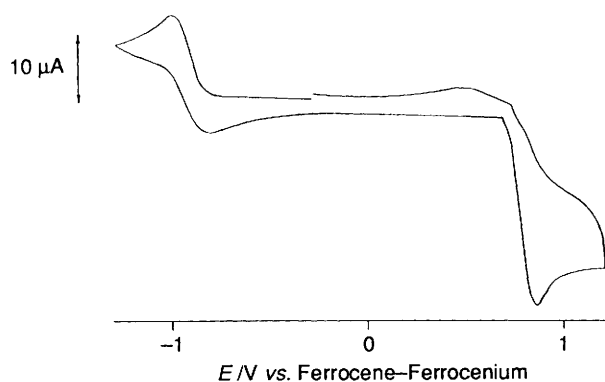


Fig. 4 Cyclic voltammogram of $[\text{CoL}_2][\text{PF}_6]$ in MeCN at 0.2 V s^{-1}

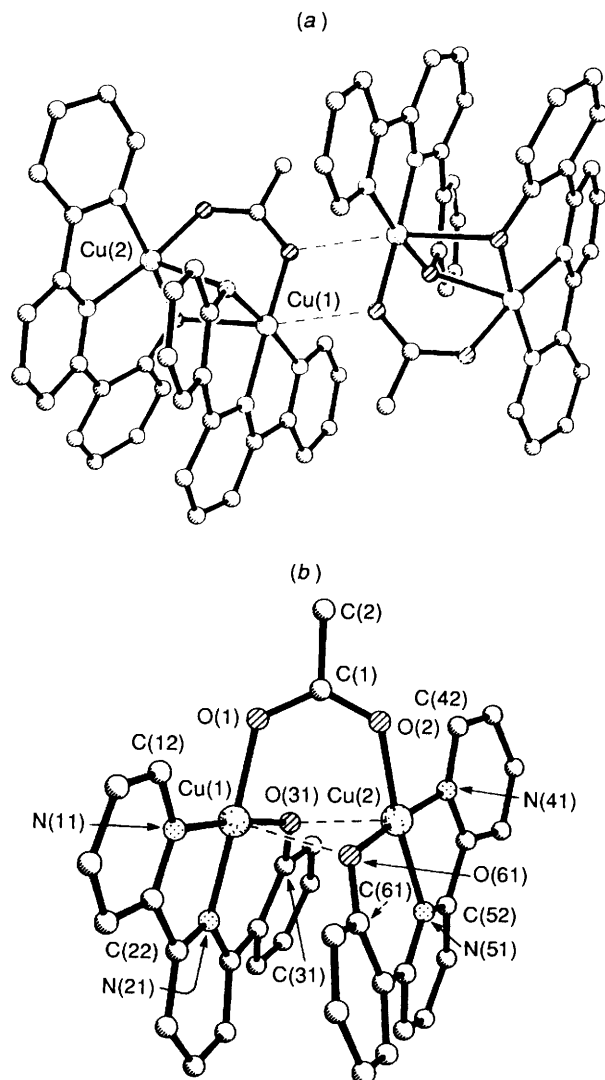


Fig. 5 Two views of the structure of the cation $[\text{Cu}_2\text{L}_2(\mu\text{-MeCO}_2)]^+$, (a) shows the interaction between binuclear units and (b) shows the atom numbering scheme and emphasises the inter-ligand π stacking

recrystallised by slow evaporation from a dichloromethane solution. The FAB mass spectrum and the elemental analysis of the desolvated material were both consistent with the rather unexpected formulation $[\text{Cu}_2\text{L}_2(\text{MeCO}_2)][\text{PF}_6]$.

The crystal structure has been determined, and contains many interesting features; two views of the complex cation are shown in Fig. 5(a) and 5(b). Relevant bond lengths and angles are in Table 4, and atomic coordinates in Table 5. The binuclear core consists of two CuL units, in which the ligand is

Table 4 Selected internuclear distances (Å) and angles ($^\circ$) for the complex $[\text{Cu}_2\text{L}_2(\mu\text{-MeCO}_2)][\text{PF}_6] \cdot 1.5\text{SCH}_2\text{Cl}_2$

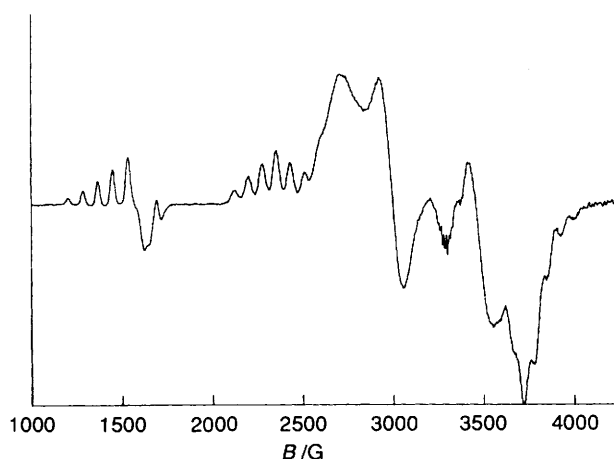
Cu(1)···Cu(2)	3.050(1)	Cu(1)–N(11)	1.977(5)
Cu(1)–O(31)	1.883(4)	Cu(1)···Cu(1a)	3.661
Cu(2)–O(2)	1.942(3)	Cu(2)–N(41)	1.981(5)
Cu(2)–O(61)	1.878(4)	C(1)–O(1)	1.265(6)
Cu(1)–O(1)	1.984(4)	Cu(1)–N(21)	1.982(5)
Cu(1)–O(61)	2.497(3)	Cu(1)–O(1a)	2.661
Cu(2)–O(31)	2.383(3)	Cu(2)–N(51)	1.974(4)
C(1)–C(2)	1.491(7)	C(1)–O(2)	1.254(5)
Cu(2)–Cu(1)–O(1)	77.4(1)	O(2)–Cu(2)–O(61)	91.2(2)
Cu(2)–Cu(1)–N(21)	104.4(1)	N(51)–Cu(2)–O(61)	94.1(2)
Cu(2)–Cu(1)–O(31)	51.4(1)	O(1)–C(1)–O(2)	125.8(5)
N(21)–Cu(1)–O(31)	93.3(2)	Cu(1)–N(11)–C(12)	126.8(4)
N(11)–Cu(1)–O(61)	89.1(1)	Cu(1)–N(21)–C(22)	112.8(3)
O(1a)–Cu(1)–O(1)	76.9	Cu(1)–O(31)–Cu(2)	90.5(1)
O(1a)–Cu(1)–O(31)	96.7	Cu(2)–N(41)–C(42)	126.6(4)
Cu(1)–Cu(2)–O(31)	38.1(1)	Cu(2)–N(51)–C(52)	112.3(4)
O(2)–Cu(2)–N(41)	91.9(2)	Cu(1)–O(61)–Cu(2)	87.2(1)
O(2)–Cu(2)–N(51)	173.5(2)	O(1)–Cu(1)–N(11)	92.9(2)
Cu(1)–Cu(2)–O(61)	54.9(1)	N(11)–Cu(1)–N(21)	82.5(2)
N(41)–Cu(2)–O(61)	176.4(1)	N(11)–Cu(1)–O(31)	173.8(1)
C(2)–C(1)–O(2)	116.8(5)	O(1)–Cu(1)–O(61)	88.9(1)
Cu(2)–O(2)–C(1)	129.2(4)	O(31)–Cu(1)–O(61)	86.4(1)
C(12)–N(11)–C(16)	119.2(5)	O(1a)–Cu(1)–N(21)	103.8
C(22)–N(21)–C(26)	120.0(5)	Cu(1)–Cu(2)–O(2)	78.6(1)
Cu(2)–O(31)–C(31)	119.1(2)	Cu(1)–Cu(2)–N(41)	127.7(1)
C(42)–N(41)–C(46)	119.8(5)	Cu(1)–Cu(2)–N(51)	107.6(1)
C(52)–N(51)–C(56)	120.6(5)	N(41)–Cu(2)–N(51)	82.7(2)
Cu(2)–O(61)–C(61)	126.1(3)	O(31)–Cu(2)–O(61)	89.9(1)
Cu(2)–Cu(1)–N(11)	125.3(1)	C(2)–C(1)–O(1)	117.4(4)
O(1)–Cu(1)–N(21)	175.3(2)	Cu(1)–O(1)–C(1)	128.4(2)
O(1)–Cu(1)–O(31)	91.3(2)	Cu(1)–N(11)–C(16)	113.7(3)
Cu(2)–Cu(1)–O(61)	37.9(1)	Cu(1)–N(21)–C(26)	126.0(4)
N(21)–Cu(1)–O(61)	90.1(1)	Cu(1)–O(31)–C(31)	126.1(4)
O(1a)–Cu(1)–N(11)	88.6	Cu(2)–N(41)–C(46)	113.6(4)
O(1a)–Cu(1)–O(61)	165.5	Cu(2)–N(51)–C(56)	124.7(3)
O(2)–Cu(2)–O(31)	91.2(1)	Cu(1)–O(61)–C(61)	120.4(3)
O(31)–Cu(2)–N(41)	91.9(2)		
O(31)–Cu(2)–N(51)	92.6(1)		

tridentate and deprotonated, stacked adjacent to one another such that the phenolates bridge the copper centres giving a Cu_2O_2 unit; the two copper(II) centres are also bridged by a μ -1,3-acetate ligand. The conformation of each ligand is similar to that already seen in $[\text{CoL}_2][\text{PF}_6]$, with considerable distortions from planarity. One independent ligand has a torsion angle of 6.5° between the two pyridyl rings, and a much larger twist in the opposite sense of 21.4° between the central pyridyl ring and the phenolate ring; in the other ligand the corresponding torsion angles are 15.0 and 21.5° with the same change of sense between them. The bite angles between the terminal N and O donor atoms in each ligand are $173.8(1)$ and $176.4(1)^\circ$, confirming that the greater flexibility of L compared to terpy allows it to confer near-ideal tetragonal geometries on metal ions {in $[\text{Cu}(\text{terpy})_2]^{2+}$ the analogous bite angle is 153.8° }.¹⁴ The Cu–N and Cu–O bond lengths to L are unremarkable; the increase of about 0.07 \AA compared to the cobalt(III) complex is simply an effect of the lower oxidation state. Apart from the N,N,O donor set of L, the basal square coordination plane of each copper(II) ion is completed by coordination of an acetate oxygen atom. The axial interactions to the bridging phenolates of the adjacent CuL fragment are rather long [$2.383(3) \text{ \AA}$ and $2.497(3) \text{ \AA}$] in keeping with the requirements of the Jahn–Teller effect.

The view of the binuclear unit shown in Fig. 5(b) emphasises the part played by the π stacking of the ligands in this structure. The two ligands are near parallel and superimposed, with a closest distance between the mean planes of stacked aromatic rings of 3.29 \AA ; the average inter-ring separation is 3.54 \AA and the largest is 4.04 \AA . These may be compared with a distance of

Table 5 Atomic coordinates ($\times 10^4$) for $[\text{Cu}_2\text{L}_2(\mu\text{-MeCO}_2)][\text{PF}_6]\cdot 1.5\text{CH}_2\text{Cl}_2$

Atom	x	y	z	Atom	x	y	z
Cu(1)	1210(1)	1274(1)	494(1)	C(33)	-997(7)	3099(4)	2601(4)
Cu(2)	4375(1)	1820(1)	2028(1)	C(34)	-1305(8)	2838(5)	3273(4)
C(1)	3235(7)	-46(3)	673(3)	C(35)	-782(8)	2089(5)	3397(4)
C(2)	3530(7)	-990(3)	316(4)	C(36)	45(7)	1605(4)	2828(3)
O(1)	1894(4)	86(2)	270(2)	N(41)	4405(6)	1494(3)	3074(3)
O(2)	4346(5)	549(2)	1349(2)	C(42)	4434(9)	660(4)	3142(4)
P	3347(3)	7380(1)	2631(1)	C(43)	4509(11)	535(5)	3917(5)
F(1)	3552(7)	6823(4)	3270(3)	C(44)	4562(13)	1280(6)	4631(5)
F(2)	4397(7)	6820(4)	2076(3)	C(45)	4510(10)	2126(5)	4556(4)
F(3)	3155(9)	7947(4)	2027(4)	C(46)	4391(7)	2210(4)	3761(3)
F(4)	2340(7)	7944(3)	3223(3)	N(51)	4577(5)	3096(3)	2831(3)
F(5)	5146(7)	8160(4)	3200(3)	C(52)	4248(7)	3077(4)	3580(3)
F(6)	1519(7)	6607(3)	2113(3)	C(53)	3766(8)	3785(4)	4122(4)
N(11)	1367(5)	1324(3)	-647(3)	C(54)	3634(8)	4537(4)	3882(4)
C(12)	1782(7)	696(4)	-1267(3)	C(55)	4032(7)	4591(4)	3136(4)
C(13)	2022(8)	852(4)	-2000(3)	C(56)	4550(7)	3859(3)	2600(3)
C(14)	1784(9)	1655(5)	-2120(4)	O(61)	4432(4)	2208(2)	1082(2)
C(15)	1350(8)	2300(4)	-1489(4)	C(61)	4995(6)	3105(3)	1117(3)
C(16)	1195(7)	2135(3)	-744(3)	C(62)	5034(7)	3903(3)	1818(3)
N(21)	588(5)	2468(3)	632(3)	C(63)	5610(8)	4805(4)	1738(4)
C(22)	857(7)	2799(3)	1(3)	C(64)	6077(9)	4909(4)	1022(5)
C(23)	860(8)	3713(4)	63(4)	C(65)	6023(8)	4126(4)	357(4)
C(24)	633(9)	4298(4)	806(4)	C(66)	5480(7)	3233(4)	395(4)
C(25)	335(8)	3967(4)	1434(4)	Cl(1)	1916(3)	3047(2)	6140(2)
C(26)	259(6)	3030(3)	1352(3)	Cl(2)	484(5)	4446(2)	5778(2)
O(31)	1207(4)	1367(2)	1630(2)	C(3)	272(14)	3564(9)	6155(8)
C(31)	379(6)	1864(3)	2129(3)	Cl(3)	8951(8)	340(4)	4556(4)
C(32)	-116(6)	2644(3)	2022(3)	C(4)	9491(33)	513(12)	5487(11)

**Fig. 6** ESR spectrum of $[\text{Cu}_2\text{L}_2(\mu\text{-MeCO}_2)][\text{PF}_6]$ as a glass in $\text{CH}_2\text{Cl}_2\text{-thf}$ (1:2) at 77 K; $G = 10^{-4} \text{ T}$

3.35 Å between the layers of graphite¹⁵ and 3.4 Å between stacked nucleotide residues in DNA.¹⁶ Interligand π -stacking interactions are also thought to play an important part in stabilising double-helical ligand arrays in complexes of polypyridines.¹ The bridging acetate is also unusual. Whilst there are very many complexes with a $\text{Cu}_2(\mu\text{-O})_2$ core, there are only a few structurally characterised examples containing an additional bridging ligand of any kind [perchlorate,¹⁷ nitrate,¹⁸ bis(diphenylphosphino)methane,¹⁹ sulfate,²⁰ trifluoromethanesulfonate²¹] and none containing an additional bridging acetate.

There is a weak association of two binuclear units in the solid state, resulting in a dimeric tetranuclear structure. This arises from a weak interaction between an acetate oxygen of one binuclear unit with a copper(II) ion of the second [dotted lines in Fig. 5(a); $\text{Cu}(1) \cdots \text{O}(1a)$ 2.661 Å]. The two binuclear units are related by a centre of symmetry. The copper(II) ions involved in this interaction [Cu(1)] are therefore in a highly elongated octahedral geometry, whereas the other copper(II) ions [Cu(2)] have elongated square-based pyramidal geometries.

The room-temperature magnetic susceptibility of $[\text{Cu}_2\text{L}_2(\text{MeCO}_2)][\text{PF}_6]$ gives an effective magnetic moment of 1.9 per Cu^{II} , which is in the range typical of magnetically dilute copper(II) ions. The ESR spectrum in a frozen $\text{CH}_2\text{Cl}_2\text{-tetrahydrofuran}$ (thf) (1:2) glass at 77 K (Fig. 6) however clearly indicates the presence of a triplet state, with a double-quantum transition at low field and a septet hyperfine coupling pattern. We are currently undertaking detailed variable-temperature ESR and magnetic susceptibility studies on this complex whose results will be reported in a future paper.²² A cyclic voltammogram of $[\text{Cu}_2\text{L}_2(\text{MeCO}_2)][\text{PF}_6]$ in CH_2Cl_2 revealed only a totally irreversible reduction at -1.2 V vs. ferrocene-ferrocenium, with several product waves between -0.3 and +0.2 V.

Reaction of HL with half an equivalent of nickel(II) acetate gave a yellow-brown solution from which a yellow solid could be precipitated on addition of KPF_6 . Recrystallisation from acetonitrile-diethyl ether yielded brown plate-like crystals. The elemental analysis is consistent with the formulation $[\text{NiL}_2]\text{-HPF}_6$; the FAB mass spectrum has a peak at $m/z = 1251$ corresponding to $[(\text{NiL}_2)_2(\text{HPF}_6)]^+$. This suggests a structure in which $[\text{NiL}_2]$ units are associated, possibly by hydrogen-bonding interactions. A crystallographic analysis is underway and the results will be reported elsewhere.

In conclusion, we have demonstrated that attachment of a phenol residue to a polypyridine ligand results in a much more varied co-ordination behaviour than might have been expected. Mixed pyridine-phenol ligands of this type clearly possess considerable potential for the synthesis of new polynuclear aggregates in which the well known co-ordination chemistry of the linear polypyridines is combined with the additional facility for polynucleation *via* the terminal phenol groups.

Acknowledgements

We thank Dr. Martin Hayes for recording the COSY spectra, Dr. Ken MacNeil for the EI mass spectra, Dr. John Maher for the ESR spectrum, the SERC Mass Spectrometry Centre at Swansea for the FAB mass spectra and the Nuffield Foundation for financial support.

References

- 1 E. C. Constable, M. D. Ward and D. A. Tocher, *J. Chem. Soc., Dalton Trans.*, 1991, 1675; E. C. Constable, M. D. Ward and D. A. Tocher, *J. Am. Chem. Soc.*, 1990, **112**, 1256; E. C. Constable, S. M. Elder, P. R. Raithby and M. D. Ward, *Polyhedron*, 1991, **10**, 1395 and refs. therein.
- 2 T. M. Garrett, U. Koert, J.-M. Lehn, A. Rigault, D. Meyer and J. Fischer, *J. Chem. Soc., Chem. Commun.*, 1990, 557; J.-M. Lehn and A. Rigault, *Angew. Chem., Int. Ed. Engl.*, 1988, **27**, 1095; J.-M. Lehn, A. Rigault, J. Siegel, J. Harrowfield, B. Chevrier and D. Moras, *Proc. Natl. Acad. Sci. USA*, 1987, **84**, 2565.
- 3 E. C. Constable, R. P. G. Henney and D. A. Tocher, *J. Chem. Soc., Dalton Trans.*, 1991, 2335; E. C. Constable, T. A. Leese and D. A. Tocher, *Polyhedron*, 1990, **9**, 1613; C. Deuschel-Cornioley, H. Stoeci-Evans and A. von Zelewsky, *J. Chem. Soc., Chem. Commun.*, 1990, 121; E. C. Constable, R. P. G. Henney, T. A. Leese and D. A. Tocher, *J. Chem. Soc., Dalton Trans.*, 1990, 443; E. C. Constable, R. P. G. Henney and T. A. Leese, *J. Organomet. Chem.*, 1989, **361**, 277.
- 4 A. Juris, V. Balzani, F. Barigoletti, S. Campagna, P. Belser and A. von Zelewsky, *Coord. Chem. Rev.*, 1988, **84**, 85; V. Balzani and F. Scandola, *Supramolecular Photochemistry*, Ellis Horwood, New York, 1991; T. J. Meyer, *Pure Appl. Chem.*, 1990, **62**, 1003 and refs. therein; G. Denti, S. Campagna, L. Sabatino, S. Serroni, M. Ciano and V. Balzani, *Inorg. Chem.*, 1990, **29**, 4750; G. Denti, S. Campagna, L. Sabatino, S. Serroni, M. Ciano and V. Balzani, *Inorg. Chim. Acta*, 1990, **176**, 175.
- 5 P. Ganis, A. Saporito, A. Vitagliano and G. Valle, *Inorg. Chim. Acta*, 1988, **142**, 75.
- 6 T. A. Geissman, M. J. Schlatter, J. D. Webb and J. D. Roberts, *J. Org. Chem.*, 1946, **11**, 741.
- 7 C. Dietrich-Buchecker and J.-P. Sauvage, *Tetrahedron*, 1990, **46**, 503.
- 8 SHELXTL PLUS program system (S320), Nicolet Instrument Corporation, 1987; SHELXTL PLUS™ program system, Siemens Analytical X-Ray instruments, 1989.
- 9 *International Tables for X-Ray Crystallography*, Kynoch Press, Birmingham, 1974, vol. 4.
- 10 T. Kaufman, J. König and A. Wolterman, *Chem. Ber.*, 1976, **109**, 3864; R. H. Fabian, D. M. Klassen and R. W. Sonntag, *Inorg. Chem.*, 1980, **19**, 1977; G. R. Newkome, D. C. Hager and F. R. Fronczek, *J. Chem. Soc., Chem. Commun.*, 1981, 858; J. M. Kelly, C. Long, C. M. O'Connell, J. G. Vos and A. H. A. Tinnemans, *Inorg. Chem.*, 1983, **22**, 2818; C. O. Dietrich-Buchecker, P. A. Marnot and J.-P. Sauvage, *Tetrahedron Lett.*, 1982, **23**, 5291; M. A. Masood, R. Jagannathan and P. S. Zacharias, *J. Chem. Soc., Dalton Trans.*, 1991, 2553.
- 11 B. N. Figgis, E. S. Kucharski and A. H. White, *Aust. J. Chem.*, 1983, **36**, 1563.
- 12 Y.-W. D. Chen, K. S. V. Santhanam and A. J. Bard, *J. Electrochem. Soc.*, 1982, **129**, 61; D. Cummins and H. B. Gray, *J. Am. Chem. Soc.*, 1977, **99**, 5158; M. C. Hughes, D. J. Macero and J. M. Rao, *Inorg. Chim. Acta*, 1981, **49**, 241; R. Prasad and D. B. Scaife, *J. Electroanal. Chem. Interfacial Electrochem.*, 1977, **84**, 373.
- 13 N. Maki, *Bull. Chem. Soc. Jpn.*, 1969, **42**, 2275.
- 14 M. I. Arriortua, T. Rojo, J. M. Amigo, G. Germain and J. P. Declercq, *Acta Crystallogr., Sect. B*, 1982, **38**, 1323.
- 15 N. N. Greenwood and A. Earnshaw, *Chemistry of the Elements*, Pergamon Press, Oxford, 1984.
- 16 *Basic Principles in Nucleic Acid Chemistry*, ed. P. O. P. Ts'O, Academic Press, New York, 1974, vol. 1.
- 17 S. K. Mandal, L. K. Thompson, M. J. Newlands and E. J. Gabe, *Inorg. Chem.*, 1989, **28**, 3707; C. J. O'Connor, D. Firmin, A. K. Pant, B. R. Babu and E. D. Stevens, *Inorg. Chem.*, 1986, **25**, 2300.
- 18 Y. N. Belokon, V. I. Tararov, T. F. Savel'eva, S. V. Vitt, E. A. Paskonova, S. C. Dotdayev, Y. A. Borisov, Y. T. Struchkov, A. S. Batasanov and V. M. Belikov, *Inorg. Chem.*, 1988, **27**, 4046; G. A. Van Albada, J. Reedijk, R. Hamalainen, U. Turpeinen and A. L. Spek, *Inorg. Chim. Acta*, 1989, **163**, 213; L. K. Thompson, F. L. Lee and E. J. Gabe, *Inorg. Chem.*, 1988, **27**, 39.
- 19 C. Floriani, P. Fiaschi, A. Chiesi-Villa, C. Guastini and P. Zanazzi, *J. Chem. Soc., Dalton Trans.*, 1988, 1607.
- 20 P. Knuuttila, *Inorg. Chim. Acta*, 1982, **58**, 201.
- 21 P. L. Dedert, T. Sorrell, T. J. Marks and J. A. Ibers, *Inorg. Chem.*, 1982, **21**, 3506.
- 22 J. P. Maher, P. Rieger, P. Thornton and M. D. Ward, unpublished work.

Received 7th February 1992; Paper 2/00677D